

A Dynamical Invariant for Sierpiński Cardioid Julia Sets*

Paul Blanchard
Daniel Cuzzocreo
Robert L. Devaney[†]
Elizabeth Fitzgibbon
Stefano Silvestri

Department of Mathematics
Boston University
111 Cummington Mall
Boston, MA 02215

April 30, 2014

*2000 MSC number: Primary 37F10; Secondary 37F45

[†]Robert L. Devaney was partially supported by Simons Foundation Grant #208870

1 Introduction

In recent years there have been a number of papers dealing with the family of rational maps

$$F_\lambda(z) = z^n + \frac{\lambda}{z^n}$$

where λ is a complex parameter. It turns out that there are several different ways that Sierpiński curves (i.e., sets homeomorphic to the Sierpiński carpet fractal) arise as Julia sets for these maps. For example, if the free critical orbits enter the basin of ∞ after iteration $\kappa \geq 3$, then it is known that the Julia set is a Sierpiński curve. In Figure 1 we display the parameter plane (the λ -plane) and a magnification near $\lambda = 0$ for this family when $n = 2$. All of the white disks in these pictures are Sierpiński holes, i.e., the Julia set corresponding to each parameter in these regions is a Sierpiński curve. So these Julia sets are all homeomorphic. There are infinitely many such holes in the parameter plane, and it is known [3], [15] that there are exactly $(n-1)(2n)^{\kappa-3}$ Sierpiński holes with escape time κ . However, only those parameters that lie in a few symmetrically located holes have topologically conjugate dynamics on their Julia sets; the dynamical behavior on Julia sets arising from other Sierpiński holes is completely different [11]. For example, when $n = 2$, only the holes that are symmetric under complex conjugation contain parameters whose associated maps are topologically conjugate on their respective Julia sets. Recently, Moreno Rocha [14] has developed a combinatorial invariant in the dynamical plane for these maps that explains why maps drawn from non-conjugate Sierpiński holes have different dynamics.

In this paper we will describe another way that Sierpiński curve Julia sets arise in these families when $n \geq 3$. For these maps, it is known that there is a McMullen domain surrounding the origin in parameter space. This domain is an open disk that contains parameters for which the Julia set is a Cantor set of

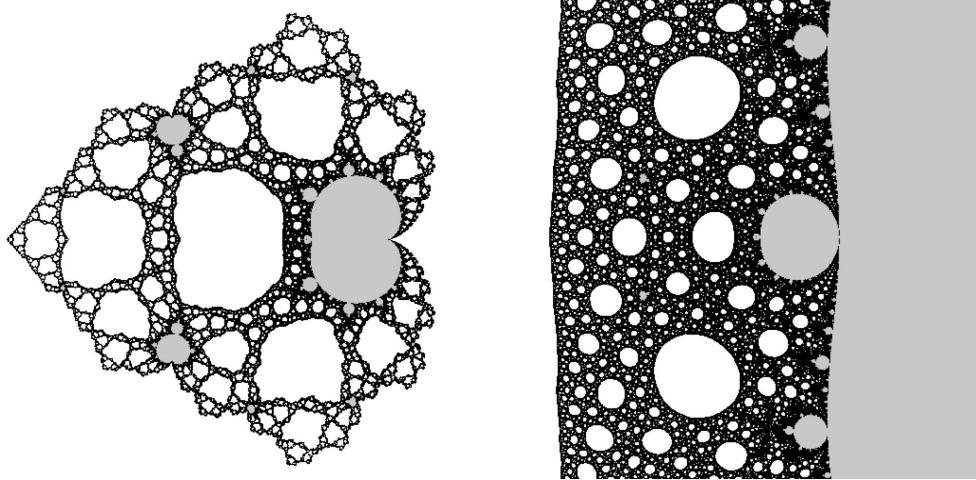


Figure 1: The parameter plane and a magnification around the origin for the family $z^2 + \lambda/z^2$. The white disks are all Sierpiński holes. The origin is located at the “tip of the tail” of the Mandelbrot set that appears to straddle the positive real axis.

simple closed curves [12]. The McMullen domain is surrounded by infinitely many disjoint closed curves \mathcal{S}_k with $k = 0, 1, \dots$ which have the property that, on each \mathcal{S}_k , there are alternately $(n-2)n^k + 1$ centers of Sierpiński holes with escape time $k+3$ and centers of main cardioids of Mandelbrot sets with base period $k+1$ [10]. These rings are therefore called *Mandelpinski necklaces*. We shall show in this paper that parameters drawn from each of the main cardioids of the Mandelbrot sets along these necklaces when $k \geq 2$ also have Julia sets that are Sierpiński curves; we therefore call these regions *Sierpiński cardioids*. For parameters in Sierpiński cardioids the dynamical behavior is quite different from the behavior that arises when the parameter lies in a Sierpiński hole. In the Sierpiński hole case, the complement of the Julia set consists of infinitely many components in which all points have orbits that eventually escape to ∞ . But in the case of the Sierpiński cardioids, there

are also infinitely many other components where orbits eventually tend to a (finite) attracting cycle. So the dynamical behavior in these Sierpiński cardioids is very different from the Sierpiński hole case. In Figure 2 we display several magnifications around the McMullen domain for the family when $n = 3$. Clearly visible in these pictures are rings around the central disk that contain numerous white regions (Sierpiński holes). But, between each pair of such disks on a given ring, there is a tiny grey region that is actually a copy of the Mandelbrot set.

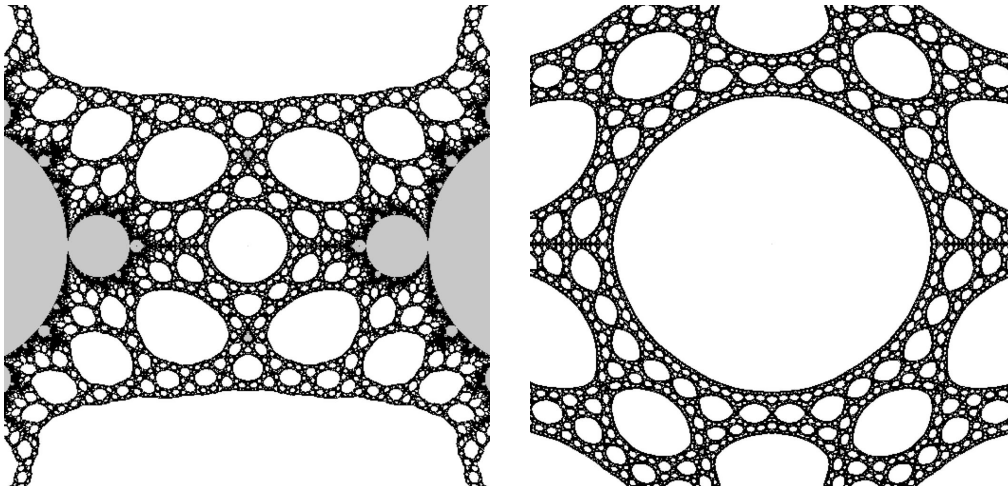


Figure 2: Magnifications of the parameter plane around the McMullen domain (the central white disk) for the family $z^3 + \lambda/z^3$.

It is known [11] that only those cardioids that are symmetrically located in the parameter plane via complex conjugation or by rotation via a certain root of unity have the same dynamics. Consequently, just as in the Sierpiński hole case, we have an exact count of the number of main cardioids along the Mandelpinski necklaces that have parameters with the same dynamics [3], [7], [10]. So the question arises: what makes parameters drawn from these non-symmetrically located cardioids have different dynamics? Another goal in

this paper is to construct a dynamical invariant for each of these parameters that specifies exactly why two parameters from different Sierpiński cardioids have non-conjugate dynamics. Roughly speaking, this invariant specifies the itinerary of the attracting cycle as it moves around relative to certain invariant Cantor necklaces that divide the Julia set into dynamically well-defined sectors.

Acknowledgement. The authors would like to thank the referee for the many excellent and thoughtful suggestions about this paper.

2 Preliminaries

Let $F_\lambda(z) = z^n + \lambda/z^n$ where $\lambda \in \mathbb{C}$ is a parameter and $n \geq 3$. When $|z|$ is large, $F_\lambda(z) \approx z^n$, so F_λ has an immediate basin of attraction at ∞ which we denote by B_λ . Each F_λ also has a pole of order n at the origin; hence there is an open neighborhood of 0 that is mapped into B_λ . Now, either this neighborhood is disjoint from the immediate basin B_λ or else this neighborhood is contained in B_λ . In the former case, we denote the entire preimage of B_λ that contains the origin by T_λ . We call this region the *trap door* since any point $z \notin B_\lambda$ for which $F_\lambda^k(z)$ lies in B_λ for some $k > 0$ has the property that there is a unique point on the orbit of z that lies in T_λ .

Besides 0 and ∞ , F_λ has $2n$ additional critical points given by $c_\lambda = \lambda^{1/2n}$. However, F_λ has only two critical values given by $v_\lambda = \pm 2\sqrt{\lambda}$ since n of the critical points are mapped to $+v_\lambda$ and the other n to $-v_\lambda$. In fact, there really is only one free critical orbit for F_λ up to symmetry. For, if n is even, we have $F_\lambda(z) = F_\lambda(-z)$ so that $F_\lambda(2\sqrt{\lambda}) = F_\lambda(-2\sqrt{\lambda})$. Therefore each of the critical orbits lands on the same point after two iterations. If n is odd, then we have $F_\lambda(-z) = -F_\lambda(z)$, so the orbits of $\pm 2\sqrt{\lambda}$ are symmetric under $z \mapsto -z$.

We call the straight rays given by tc_λ with $t > 0$ the *critical point rays*. Note that

$$F_\lambda(tc_\lambda) = \lambda^{1/2} \left(t^n + \frac{1}{t^n} \right),$$

so it follows easily that each critical point ray is mapped two-to-one onto the straight ray tv_λ with $t \geq 1$ that extends from v_λ to ∞ . We call this ray the *critical value ray*. Each F_λ also has $2n$ prepoles p_λ given by $p_\lambda = (-\lambda)^{1/2n}$, so $F_\lambda(p_\lambda) = 0$. Note that all of the critical points and prepoles lie on the circle of radius $|\lambda|^{1/2n}$ centered at the origin. We call this circle the *critical circle*. One checks easily that F_λ maps the critical circle $2n$ -to-1 onto the straight line segment connecting $\pm v_\lambda$ and passing through the origin. We call this line segment the *critical segment*.

Recall that the *Julia set* $J(F_\lambda)$ for the rational map F_λ has several equivalent characterizations. It is known [13] that the Julia set is the closure of the set of repelling periodic points as well as the boundary of the set of points whose orbits tend to ∞ . $J(F_\lambda)$ is also the set of points in \mathbb{C} at which the family of iterates $\{F_\lambda^n\}$ is not a normal family in the sense of Montel.

There are several symmetries in the dynamical plane. First, let $\omega = \exp(\pi i/n)$. Then we have $F_\lambda(\omega z) = -F_\lambda(z)$, so, as above, either the orbits of z and ωz coincide after two iterations (when n is even), or else they behave symmetrically under $z \mapsto -z$ (when n is odd). In either event, the dynamical plane and the Julia set both possess $2n$ -fold symmetry, as do B_λ and T_λ . Let $H_\lambda(z)$ be one of the n involutions given by $\lambda^{1/n}/z$. Then $F_\lambda(H_\lambda(z)) = F_\lambda(z)$, so the dynamical plane and Julia set are also symmetric under each H_λ . Note that $H_\lambda(B_\lambda) = T_\lambda$.

The following result was proved in [9].

Theorem (*The Escape Trichotomy*). *Let $F_\lambda(z) = z^n + \lambda/z^n$ and consider the orbit of the critical value v_λ .*

1. If v_λ lies in B_λ , then $J(F_\lambda)$ is a Cantor set;
2. If v_λ lies in T_λ , then $J(F_\lambda)$ is a Cantor set of disjoint simple closed curves, each of which surrounds the origin;
3. If $F_\lambda^k(v_\lambda)$ lies in T_λ where $k \geq 1$, then $J(F_\lambda)$ is a Sierpiński curve.

Finally, if v_λ does not lie in either B_λ or T_λ , then $J(F_\lambda)$ is a connected set.

We remark that case 2 of the above result was proved by McMullen [12]. This part of the Theorem does not hold if $n = 1$ or $n = 2$; this is one of the reasons we restrict attention in this paper to the case $n \geq 3$.

A *Sierpiński curve* is any planar set that is homeomorphic to the well-known fractal called the *Sierpiński carpet*. By a result of Whyburn [18], there is a topological characterization of any such set: any planar set that is compact, connected, locally connected, nowhere dense, and has the property that any pair of complementary domains are bounded by simple closed curves that are pairwise disjoint is known to be homeomorphic to the Sierpiński carpet.

We turn now to the parameter plane for these families, i.e., the λ -plane. There are two different symmetries in the parameter planes for these maps. First, F_λ and $F_{\bar{\lambda}}$ are easily seen to be conjugate via $z \mapsto \bar{z}$. Hence the parameter plane is symmetric under complex conjugation. Second, let $\nu = \exp(2\pi i/(n-1))$. Then we have $\nu F_\lambda(z) = F_{\nu^2 \lambda}(\nu z)$ so the parameters λ and $\nu^{2j} \lambda$ correspond to maps that have conjugate dynamics. Thus the parameter plane is also symmetric under the rotation $\lambda \mapsto \nu^2 \lambda$. In particular, if n is even, then all parameters of the form $\nu^j \lambda$ have conjugate dynamics, but if n is odd, it is known [11] that the parameters λ and $\nu^{2j+1} \lambda$ do not have conjugate dynamics.

In fact, the parameter plane actually is symmetric under the rotation $\lambda \mapsto \nu \lambda$, although, when n is odd, this symmetry is no longer given by a

conjugacy between F_λ and $F_{\nu\lambda}$. One computes easily that

$$F_{\nu\lambda}(\nu^{1/2}z) = -\nu^{1/2}(F_\lambda(z)).$$

Since $F_\lambda(-z) = -F_\lambda(z)$ when n is odd, it follows that $F_{\nu\lambda}^2$ is conjugate to F_λ^2 via the map $z \mapsto \nu^{1/2}z$ when n is odd. This means that the dynamics of F_λ and $F_{\nu\lambda}$ are “essentially” the same, though subtly different. For example, if F_λ has a fixed point, then under the conjugacy, this fixed point and its negative (which is also fixed) are mapped to a 2-cycle for $F_{\nu\lambda}$. Nevertheless, the Julia sets of F_λ and $F_{\nu\lambda}$ are homeomorphic under $z \mapsto \nu^{1/2}z$, and so this implies that the parameter plane for n odd is also symmetric under the rotation $\lambda \mapsto \nu\lambda$. The parameter plane can thus be separated into $n - 1$ symmetry sectors \mathcal{P}_j , $j = 0, \dots, n - 2$, given by

$$\frac{2j\pi}{n-1} \leq \text{Arg } \lambda < \frac{2(j+1)\pi}{n-1}.$$

The boundary curves of these sectors contain parameters for which the critical values lie on a pair of critical rays.

Because of the Escape Trichotomy, the parameter plane for F_λ divides into three distinct regions. Let \mathcal{L} be the set of parameters for which $v_\lambda \in B_\lambda$ so $J(F_\lambda)$ is a Cantor set. We call \mathcal{L} the *Cantor set locus*. As in the case of the Mandelbrot set and quadratic polynomials, there is a well defined Böttcher coordinate Φ defined on \mathcal{L} . It is known [16] that $\Phi : \mathcal{L} \rightarrow \mathbb{C} - \overline{\mathbb{D}}$ is an analytic homeomorphism and that the preimages of all straight rays in $\mathbb{C} - \overline{\mathbb{D}}$ land on a unique point in the boundary of \mathcal{L} and that the boundary of \mathcal{L} is a simple closed curve surrounding 0 in the parameter plane.

Let \mathcal{M} denote the set of parameters for which $v_\lambda \in T_\lambda$; \mathcal{M} is called the *McMullen domain*. It is known [2] that \mathcal{M} is an open disk punctured at the origin and bounded by a simple closed curve.

Let \mathcal{C} denote the complement of $\mathcal{L} \cup \mathcal{M}$. \mathcal{C} is called the *connectedness locus* since $J(F_\lambda)$ is a connected set if $\lambda \in \mathcal{C}$. It is known [3], [15] that \mathcal{C}

contains precisely $(n - 1)(2n)^{\kappa-3}$ *Sierpiński holes* with escape time $\kappa \geq 3$. These are open disks in \mathcal{C} in which each corresponding map has the property that the critical orbit lands in B_λ at iteration κ or, equivalently, the orbit of the critical value lands in T_λ at iteration $\kappa - 2$. See Figure 3. Each of these Sierpiński holes is also known to be bounded by a simple closed curve [16].

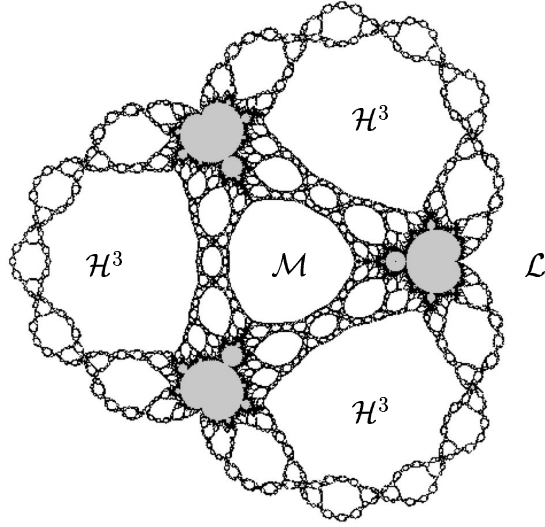


Figure 3: The parameter plane when $n = 4$. The open disks marked \mathcal{H}^3 are the Sierpiński holes with escape time 3.

In Figure 3, there are three clearly visible copies of the Mandelbrot set. Indeed, it is known [4] that there are $n - 1$ copies of the Mandelbrot set that straddle the rays given by $\text{Arg } \lambda = t\nu^k$ for $t > 0$. These sets are called the *principal Mandelbrot sets* in the parameter plane. The cusps of the main cardioids of these sets all lie on the boundary of \mathcal{L} while the tips of the tails of these sets (i.e., the parameters corresponding to $c = -2$ in the usual Mandelbrot set for $z^2 + c$) all lie on the boundary of \mathcal{M} .

3 Rings around the McMullen Domain

In this section, we give a brief sketch of the proof that the McMullen domain is surrounded by infinitely many disjoint simple closed curves \mathcal{S}_k , $k = 0, 1, 2, \dots$ with the \mathcal{S}_k converging down to the boundary of the McMullen domain as $k \rightarrow \infty$. Each \mathcal{S}_k contains exactly $(n - 2)n^k + 1$ parameter values that are the centers of Sierpiński holes with escape time $k + 3$ and the same number of centers of main cardioids of Mandelbrot sets with base period $k + 1$, i.e., Sierpiński cardioids. By a center of a Sierpiński hole, we mean the (unique) parameter in this disk for which the critical orbit lands on ∞ rather than being attracted to ∞ . Also, base period ℓ means that the critical orbits first return to the critical circle at iteration ℓ . This does not necessarily mean that the parameters drawn from such a Sierpiński cardioid have an attracting cycle of period ℓ . Rather, when n is odd, two critical points $\pm c_\lambda$ may each return to their negatives when they first return to the critical circle. Thus, when this occurs, the orbit of $\pm c_\lambda$ is periodic of period 2ℓ . This happens, for example, in the principal Mandelbrot set centered along the negative real axis when n is odd. Here parameters drawn from the main cardioid have period 2 cycles although the base period is 1.

There is one exception to the statement that these parameters lie at the centers of main cardioids of Mandelbrot sets: the curve \mathcal{S}_1 passes through $n - 1$ centers of period 2 bulbs in the principal Mandelbrot sets instead of the centers of main cardioids of Mandelbrot sets with base period 2. Here the period 2 bulb is the largest hyperbolic component attached to the main cardioid of the principal Mandelbrot sets; as above, parameters in this bulb have an attracting cycle of period either 2 or 4 depending upon the period of the main cardioid.

For simplicity, we shall restrict attention in this section to the case $n = 3$;

the minor adjustments necessary for the case $n > 3$ will be described at the end of this section. The proof for the general case may also be found in [10], but the proof we give here is somewhat simpler.

Recall that the critical circle in the dynamical plane is given by $|z| = |\lambda|^{1/6}$ and that F_λ maps this circle 6-to-1 onto the critical segment, i.e., the straight line segment connecting $\pm v_\lambda = \pm 2\sqrt{\lambda}$. We denote this circle by $C_0 = C_0(\lambda)$. We assume throughout this section that $|v_\lambda| < |\lambda|^{1/6}$, so this implies that the critical segment lies in the interior of the disk bounded by the critical circle. As we shall see, this condition will be essential to proving the existence of the rings \mathcal{S}_k . Let \mathcal{O} be the set of nonzero parameters for which this holds. Thus we have $|2\sqrt{\lambda}| < |\lambda|^{1/6}$ for $\lambda \in \mathcal{O}$, so it follows that \mathcal{O} is the open disk of radius $1/8$ centered at the origin. For $\lambda \in \mathcal{O}$, F_λ maps the exterior of the critical circle as a 3-to-1 covering onto the exterior of the critical segment. Thus there is a simple closed curve in the exterior of C_0 that is mapped 3-to-1 onto C_0 . Call this curve $C_1 = C_1(\lambda)$. Since the exterior of C_1 is then mapped onto the exterior of C_0 as an 3-to-1 covering, there is another simple closed curve $C_2 = C_2(\lambda)$ that lies outside C_1 and is mapped 3-to-1 onto C_1 . Continuing in this fashion, we find an infinite collection of simple closed curves $C_k = C_k(\lambda)$ for $k > 0$ satisfying $F_\lambda(C_{k+1}) = C_k$ and hence $F_\lambda^k(C_k) = C_0$. Note that the C_k are all disjoint and it can be shown that they converge outward to ∂B_λ as $k \rightarrow \infty$.

Since the interior of the critical circle is also mapped as a 3-to-1 covering of the exterior of the critical segment, there are other simple closed curves $C_{-k} = C_{-k}(\lambda)$ for $k = 1, 2, \dots$ such that F_λ maps C_{-k} as a 3-to-1 covering of C_{k-1} just as above. The C_{-k} now converge down to ∂T_λ as $k \rightarrow \infty$. Since C_0 contains 6 critical points and 6 prepoles, it follows that each C_k contains $2 \cdot 3^{|k|+1}$ points that map under F_λ^k onto the critical points and the same number of points that map to the prepoles. The critical points and prepoles

are arranged in alternate fashion around C_0 , so their preimages on the C_k are arranged similarly.

We now describe the ring \mathcal{S}_0 in the parameter plane. This curve consists of λ -values for which the critical values lie on the critical circle C_0 in the dynamical plane. So, on this set, we must have $|\lambda|^{1/6} = 2|\sqrt{\lambda}|$. As above, solving this equation shows that \mathcal{S}_0 is the circle of radius $1/8$ in the parameter plane. We call \mathcal{S}_0 the *dividing circle* in the parameter plane. When $\lambda \in \mathcal{S}_0$, the critical circle in the dynamical plane is the circle of radius $1/\sqrt{2}$ centered at the origin. Note that, as λ rotates around the dividing circle in a certain direction, the critical points rotate around the critical circle C_0 by $1/6$ of a turn while the critical values rotate by half a turn in the same direction as λ rotates. It then follows easily that there are a pair of parameters on the dividing circle for which the critical values land on a pair of critical points (these give the centers of the two principal Mandelbrot sets with base period 1) and a pair where they land on the prepoles $(-\lambda)^{1/6}$ (these are centers of Sierpiński holes). This gives the result for \mathcal{S}_0 . Note that the parameters in \mathcal{O} are precisely those that lie inside the dividing circle \mathcal{S}_0 .

For $\lambda \in \mathcal{O}$ with $0 \leq \text{Arg } \lambda < 2\pi$, let $c_0 = \lambda^{1/6}$ denote the critical point satisfying $0 \leq \text{Arg } c_0 < \pi/3$ and let c_1, \dots, c_5 denote the other critical points where the c_j are arranged in the counterclockwise direction around the origin. Let I_0 denote the closed sector in \mathbb{C} bounded by the two critical point rays that are given by tc_0 and tc_5 with $t \geq 0$. We call this sector a *prepole* sector since there is a unique prepole in the “center” of I_0 . Let I_j denote the similar prepole sector bounded by tc_{j-1} and tc_j . Note that the interior of each I_j is mapped one-to-one onto \mathbb{C} minus the two critical value rays tv_λ where $t \geq 1$. One of the critical point rays that bounds each I_j is mapped onto one of these critical value rays while the other critical point ray is mapped to the other critical value ray. If $\text{Arg } \lambda = 0$ then the critical value rays lie in $I_0 \cap I_1$

and $I_3 \cap I_4$, whereas, if we allow $\text{Arg } \lambda$ to increase to 2π , the critical value rays now lie in $I_2 \cap I_3$ and $I_0 \cap I_5$. When $\lambda \notin \mathbb{R}^+$, the critical value rays lie in the interior of $I_1 \cup I_2$ and $I_4 \cup I_5$. In particular, if $\lambda \notin \mathbb{R}^+$, then the critical value rays do not meet I_0 or I_3 .

We now define a parametrization of each C_k which we shall denote by $C_k(\theta)$. Each $C_k(\theta)$ will be $3^{|k|} \cdot 2\pi$ periodic. We begin by parametrizing C_0 . We set $C_0(0)$ to be the point of intersection of the critical circle C_0 and $I_0 \cap I_1$, i.e., the critical point c_0 . Since C_0 is an actual circle, we may then parametrize C_0 in the natural way; however, for reasons that will become clearer later, we choose to make this parametrization increase in the clockwise direction around the origin rather than the conventional counterclockwise direction. So the parametrization $C_0(\theta)$ is periodic with period 2π .

Now C_1 is mapped 3-to-1 onto C_0 , so we define $C_1(0)$ to be the unique point in the region I_0 that is mapped to $C_0(0)$ provided that $\lambda \notin \mathbb{R}^+$. If $\lambda \in \mathbb{R}^+$, we choose $C_1(0)$ to be the preimage of $C_0(0)$ that lies in \mathbb{R}^+ and outside C_0 . So $C_1(0)$ depends continuously on λ provided that $0 \leq \text{Arg } \lambda < 2\pi$. Then we define $C_1(\theta)$ to be the point in C_1 that is mapped to $C_0(\theta)$ where we choose $C_1(\theta)$ so that this function is continuous in θ . Since C_1 is mapped 3-to-1 onto C_0 , it follows that $C_1(\theta)$ is $3 \cdot 2\pi$ periodic in θ . Note that this also parametrizes C_1 in the clockwise direction. Then we continue inductively for $k > 1$ by first defining $C_k(0)$ as above to be the unique point in I_0 that is mapped to $C_{k-1}(0)$ (with a similar modification if $\lambda \in \mathbb{R}^+$), and then we extend this by defining $C_k(\theta)$ to be the unique point that is mapped to $C_{k-1}(\theta)$ and so that this map is continuous in θ . Therefore C_k is $3^k \cdot 2\pi$ periodic in θ . To define $C_{-k}(\theta)$, recall that there is an involution $H_\lambda(z) = \lambda^{1/3}/z$ for which $F_\lambda(H_\lambda(z)) = F_\lambda(z)$. Here we choose the involution H_λ that fixes $c_0(\lambda)$. Then we define $C_{-k}(\theta) = H_\lambda(C_k(\theta))$. Note that this parametrizes C_{-k} in the counterclockwise direction, which is the reason why

we chose to parametrize $C_0(\theta)$ in the clockwise direction. So $C_{-k}(\theta)$ is $3^{|k|} \cdot 2\pi$ periodic in θ .

We shall now consider only portions of the curves C_k . Let γ_0 denote the portion of C_0 defined for $0 \leq \theta \leq 4\pi/3 = 3^0\pi + \pi/3$. Note that γ_0 extends from the boundary of $I_0 \cap I_1$ in the clockwise direction to the boundary of $I_2 \cap I_3$, i.e., two-thirds of a turn in the clockwise direction. The curve γ_0 therefore extends in the clockwise direction from the critical point c_0 to c_2 and passes through c_5, c_4 , and c_3 . For $k > 0$ let γ_k denote the portion of C_k defined for $0 \leq \theta \leq 3^k\pi + \pi/3$. For each k we then have that $\gamma_k(0)$ lies in I_0 .

For later use, note that the point $z_k = \gamma_k(\pi/6)$ also lies in I_0 for each k . The forward orbit of z_k lies in I_0 until this orbit reaches 0, and $F_\lambda^k(z_k)$ is thus the unique prepole in I_0 . The points z_k will be points that lie in the invariant Cantor necklace that we shall define in the next section.

Since C_k is $3^k \cdot 2\pi$ -periodic and γ_k is defined only for $0 \leq \theta \leq 3^k\pi + \pi/3$, we have that γ_k occupies a little more than one-half of the full curve C_k . In particular, we have $\gamma_k(3^k\pi) = -\gamma_k(0)$ by the $z \mapsto -z$ symmetry, and so, for each k , $\gamma_k(3^k\pi)$ lies in I_3 and is mapped to $c_3 = \gamma_0(\pi)$ by F_λ^k . Since $F_\lambda^k(\gamma_k(0)) = c_0$, it follows that the other endpoint $\gamma_k(3^k\pi + \pi/3)$ also lies in the sector I_3 and is mapped to $\gamma_0(4\pi/3) = c_2$ by F_λ^k since, for each k , we have

$$F_\lambda^k(\gamma_k(3^k\pi + \pi/3)) = \gamma_0(3^k\pi + \pi/3) = \gamma_0(\pi + \pi/3).$$

Hence, γ_k is a curve that passes clockwise through a portion of I_0 , then through all of I_5 and I_4 , and finally through a portion of I_3 as θ increases. Note also by the $z \mapsto -z$ symmetry, $\gamma_k(3^k\pi + \pi/6)$ also lies in I_3 for each k and $F_\lambda^k(\gamma_k(3^k\pi + \pi/6))$ is the unique prepole in I_3 . These are points that lie in the opposite portion of the Cantor necklace defined in Section 4.

We now define $\gamma_{-k}(\theta)$ for $k > 0$; this definition will be somewhat different from that of $\gamma_k(\theta)$ when $k > 0$. First note that F_λ maps the portion of C_{-1}

that lies in $I_1 \cup I_2$ onto the entire circle C_0 . The two endpoints of this portion of C_{-1} are sent to the same point on the critical value ray that lies in $I_1 \cup I_2$. Hence there is an arc in C_{-1} that is a preimage of γ_0 under F_λ in $I_1 \cup I_2$. We define $\gamma_{-1}(\theta)$ to be this preimage of $\gamma_0(\theta)$ under F_λ . So $\gamma_{-1}(\theta)$ is defined for $0 \leq \theta \leq 3^0\pi + \pi/3$, just as $\gamma_0(\theta)$ is. Continuing in similar fashion, we let $\gamma_{-k}(\theta)$ be the point lying on the portion of the curve C_{-k} in $I_1 \cup I_2$ that is mapped by F_λ to $\gamma_{k-1}(\theta)$. So $\gamma_{-k}(\theta)$ is defined for $0 \leq \theta \leq 3^{k-1}\pi + \pi/3$, just as γ_{k-1} is. See Figure 4.

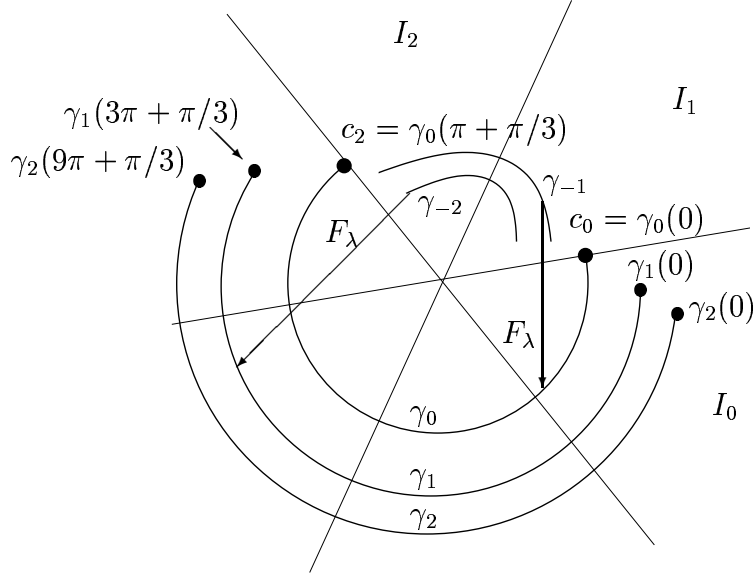


Figure 4: The curves γ_k .

Proposition. *When $\text{Arg } \lambda = 0$ and $k > 0$, all of the points $\gamma_{-k}(0)$ lie in \mathbb{R}^+ . When $\text{Arg } \lambda = 2\pi$, the endpoints of γ_{-k} corresponding to $\theta = 3^{k-1}\pi + \pi/3$ lie in \mathbb{R}^- .*

Proof: The first part of the result follows immediately from the definition of $\gamma_{-k}(0)$. As $\text{Arg } \lambda$ increases by 2π , the point c_0 rotates a sixth of a turn

in the counterclockwise direction and so the point $\gamma_0(\pi + \pi/3)$ now lies on \mathbb{R}^- . Since \mathbb{R}^- is invariant when $\text{Arg } \lambda = 2\pi$, it then follows that each of the endpoints of γ_{-k} with $\theta = 3^{k-1}\pi + \pi/3$ also lies in \mathbb{R}^- .

□

We now define the rings \mathcal{S}_k for $k > 0$ in the parameter plane. Recall that \mathcal{O} is the set of nonzero parameters for which v_λ lies inside the critical circle. Let \mathcal{D}_r be a closed disk of radius $r > 0$ surrounding the origin and lying strictly inside the McMullen domain. Let $\tilde{\mathcal{O}} = \mathcal{O} - (\mathcal{D}_r \cup \mathbb{R}^+)$. Note that $\tilde{\mathcal{O}}$ is a simply connected open set. Let $\theta_k = 3^{k-1}\pi + \pi/3$, so $\gamma_{-k}(\theta)$ is defined for θ in the interval $[0, \theta_k]$.

Proposition. *Suppose $\lambda \in \tilde{\mathcal{O}}$ and let v_λ denote the critical value of F_λ that lies in the upper half plane. Fix $k \geq 1$ and θ in the open interval $(0, \theta_k)$. Then there is a unique $\lambda = \lambda_\theta^k$ in $\tilde{\mathcal{O}}$ for which the critical value v_λ lands on $\gamma_{-k}(\theta)$. Moreover, λ_θ^k varies continuously with θ .*

Proof: For each θ in $(0, \theta_k)$, we have two maps defined on the region $\tilde{\mathcal{O}}$ in the parameter plane. The first map is $V(\lambda) = v_\lambda$ where v_λ is the unique critical value in the upper half plane. Since the outer boundary of $\tilde{\mathcal{O}}$ is the dividing circle $|\lambda| = 1/8$, it follows that V_λ maps $\tilde{\mathcal{O}}$ univalently onto the open region D given by $|z| < 1/\sqrt{2}$ and $\text{Im } z > 0$ minus a small half-disk around the origin. Hence V^{-1} is well defined on D .

The second map defined on $\tilde{\mathcal{O}}$ is the map $\mu_\theta(\lambda) = \gamma_{-k}(\theta)$ where θ is a given value in the open interval $(0, \theta_k)$. Hence μ maps all parameters in $\tilde{\mathcal{O}}$ strictly inside the region D , since for each λ , $\gamma_{-k}(\theta)$ lies strictly inside $C_0(\lambda)$ and outside T_λ . In particular, $\mu_\theta(\lambda)$ is bounded away from 0 since $|\lambda| > r$. Consequently the map $V^{-1} \circ \mu_\theta$ takes $\tilde{\mathcal{O}}$ strictly inside itself. By the Schwarz Lemma, $V^{-1} \circ \mu_\theta$ has a unique fixed point in $\tilde{\mathcal{O}}$. This is the parameter λ_θ^k , which then varies continuously with θ in the open interval $(0, \theta_k)$.

□

To complete the construction of the ring \mathcal{S}_k , we next show that the curve $\theta \mapsto \lambda_\theta^k$ becomes a simple closed curve when we add in the endpoints of $[0, \theta_k]$.

Proposition. *The parameter λ_θ^k varies continuously with θ . As $\theta \rightarrow 0$ (resp., $\theta \rightarrow \theta_k$), λ_θ^k tends to a unique parameter λ_0^k (resp., $\lambda_{\theta_k}^k$) in \mathbb{R}^+ for which the critical value in the upper half plane lands on $\gamma_{-k}(0) \in \mathbb{R}^+$ (resp., $\gamma_{-k}(\theta_k) = -\gamma_{-k}(0) \in \mathbb{R}^-$). Furthermore, $\lambda_0^k = \lambda_{\theta_k}^k \in \mathbb{R}^+$, so $\theta \mapsto \lambda_\theta^k$ is a simple closed curve.*

Proof: To prove this, we modify the parameterizations of the curves γ_k and the domain in the parameter plane on which the two maps $V(\lambda)$ and $\mu_\theta(\lambda)$ are defined. First, let $\hat{\mathcal{O}} = \mathcal{O} - (\mathcal{D}_r \cup \mathbb{R}^-)$. So $\hat{\mathcal{O}}$ is also a simply connected open set in \mathbb{C} . Then the map $V(\lambda)$ is now the critical value that lies in the right half plane. Then let γ_0 be the portion of the critical circle defined for $0 \leq |\theta| < \pi/2 + \pi/6$. So γ_0 now lies in the sectors I_0, I_1, I_2 , and I_5 . Then define γ_k for $k > 0$ to be the portion of C_k defined for $0 \leq |\theta| < 3^k\pi/2 + \pi/6$. So these new γ_k 's are just rotations of the previously defined curves. Then we define γ_{-k} to be the portion of the preimage of γ_{k-1} that resides in $I_0 \cup I_1$.

Then one checks easily that, as above, when $\lambda \in \hat{\mathcal{O}}$, the map $\mu_\theta^k(\lambda)$ now takes values in the open region \hat{D} given by $|z| < 1/\sqrt{2}$ and $\operatorname{Re} z > 0$ minus a small half-disk in the upper half-plane centered at the origin, which is again the image of $\hat{\mathcal{O}}$ under V . Then the previous proof reproduces a continuous curve of parameters λ_θ^k for which the critical value lies at $\mu_\theta(\lambda)$.

Now suppose that $\operatorname{Arg} \lambda = 0$. By the earlier Proposition, each $\gamma_k(0)$ lies in \mathbb{R}^+ . Moreover, using standard results from real dynamics in the Mandelbrot set, there is a unique superstable parameter for which we have

$$v_\lambda < c_0 = F_\lambda^k(c_0) < F_\lambda^{k-1}(c_0) < \dots < F_\lambda^2(c_0).$$

This then is the parameter λ_0^k . Since the new points λ_θ^k vary continuously

with θ , this shows that the earlier parametrization defined for $0 < \theta < \theta_k$ extends continuously to $\lambda_0^k \in \mathbb{R}^+$.

When $\text{Arg } \lambda = 2\pi$, a similar modification of the proof of the previous Proposition shows that we again have a unique parameter for which the orbit of v_λ lies in \mathbb{R}^- and we have

$$0 > v_\lambda > c_2 = F_\lambda^k(c_2) > F_\lambda^{k-1}(c_2) > \dots > F_\lambda^2(c_2).$$

This is the parameter $\lambda_{\theta_k}^k$, using the parametrization from the previous Proposition. Since we have symmetric behavior on \mathbb{R}^+ , it follows that $\lambda_0^k = \lambda_{\theta_k}^k$. By continuity, as $\text{Arg } \lambda \rightarrow 0$ or 2π , the parameters λ_θ^k converge to $\lambda_0^k = \lambda_{\theta_k}^k$. Therefore the parameters λ_θ^k lie along a simple closed curve surrounding the origin in the parameter plane.

□

We therefore define the ring \mathcal{S}_k in the parameter plane to be the curve given by $\theta \mapsto \lambda_\theta^k$. So \mathcal{S}_1 consists of parameters for which the critical points first map to the critical values which lie inside the critical circle, and then the critical values map back onto the critical circle. For $k > 1$, \mathcal{S}_k consists of parameters for which the critical points again map inside the critical circle. But then the next images lie outside the critical circle. And then these orbits remain outside the critical circle for $k - 1$ more iterations until landing back on the critical circle at iteration $k + 1$.

From the results in [3], it is known that the parameters in \mathcal{S}_k for which the critical orbit lands on a critical point at iteration $k + 1$ lie at the centers of the main cardioid of Mandelbrot sets with base period $k + 1$ (with two exceptions on the ring \mathcal{S}_1 where they lie at the centers of the period 2 bulb of the principal Mandelbrot sets). These parameters are given by λ_θ^k where $\theta = \ell\pi/3$ where ℓ is an integer with $0 \leq \ell \leq 3^k$. We therefore denote these special parameters by λ_ℓ^k . Thus there are exactly $3^k + 1$ such parameters

along \mathcal{S}_k .

As we will show in Section 5, the Julia sets corresponding to parameters in the main cardioids of these Mandelbrot sets are all Sierpiński curves (when $k > 1$), and hence they are all homeomorphic to one another. It is known that any two parameters drawn from the same Sierpiński cardioid have conjugate dynamics on their Julia sets. It is also known [11] that only those parameters that are drawn from a given cardioid or the complex conjugate cardioid have conjugate dynamics on their Julia sets. All other parameters drawn from different Sierpiński cardioids necessarily have distinct dynamical behavior. This result follows from Thurston's Theorem [11]. In Section 7, we produce a dynamical invariant that shows why these non-complex conjugate cardioids have non-conjugate dynamics. For this it will suffice to provide a dynamical invariant for the parameters at the centers of these cardioids, i.e., for the λ_ℓ^k .

We now describe the minor modifications of the above proof needed to prove the existence of the rings \mathcal{S}_k when $n > 3$. The proof of the existence of \mathcal{S}_0 is exactly as above, only now this dividing circle is the circle of radius $2^{-2n/(n-1)}$ centered at the origin, and it contains $n - 1$ parameters for which the critical values land on critical points and the same number for which they land on prepoles.

When $n > 3$, there are now $2n$ critical points and prepoles, and the curves C_k are mapped n -to-1 onto their images. There are also $2n$ prepole sectors and we may define I_j for $j = 0, \dots, n - 1$ and $C_k(\theta)$ for $k > 0$ exactly as above. We then choose the portions $\gamma_k(\theta)$ in C_k for $k > 0$ to be defined for $0 \leq \theta \leq (n - 2)n^k\pi + \pi/n$. Note that these portions of C_k now wind further around the origin than they did in the case $n = 3$. For example, when $n = 4$, each $\gamma_k(\theta)$ winds a little more than once around the origin; when $n = 5$, each $\gamma_k(\theta)$ winds a little more than one and a half times around the origin. We again let $\gamma_{-k}(\theta)$ be the preimage of $\gamma_{k-1}(\theta)$, but this time $\gamma_{-k}(\theta)$ lies in

$I_1 \cup \dots \cup I_{n-1}$. Note that, as λ rotates once around the origin, the sectors $I_1 \cup \dots \cup I_{n-1}$ remain as before in the upper half plane. Then the previous proof again produces the parameters λ_θ^k that define \mathcal{S}_k .

As earlier, the point $z_k = \gamma_k(\pi/2n)$ also lies in I_0 for each k . So the forward orbit of z_k again lies in I_0 until this orbit reaches 0, and $F_\lambda^k(z_k)$ is the unique prepole in I_0 .

4 Dynamical Sectors

In the previous section, we used the prepole sectors I_j to construct the rings \mathcal{S}_k around the McMullen domain in the parameter plane for

$$F_\lambda(z) = z^n + \frac{\lambda}{z^n}$$

where $n \geq 3$. Each of these rings passed through a number of centers of Sierpiński cardioids. We shall prove in Section 5 that the Julia set corresponding to each parameter drawn from one of these cardioids when $k > 1$ is always a Sierpiński curve, and hence all of these Julia sets are homeomorphic. However, only certain symmetrically located cardioids contain parameters that have conjugate dynamics. To produce a dynamical invariant that shows why parameters from certain Sierpiński cardioids have non-conjugate dynamics, we need to construct different sectors that are more dynamically defined. The boundaries of these sectors will include objects known as Cantor necklaces.

To define a Cantor necklace, we begin with the special case called the Cantor middle-thirds necklace. This set is the subset of the plane constructed as follows. Start with the Cantor middle-thirds set lying in the unit interval on the x -axis. Then adjoin open disks in place of each of the removed open intervals along this axis. The resulting set is the Cantor middle-thirds

necklace. Then a Cantor necklace is any planar set that is the image of the middle-thirds necklace under a continuous, one-to-one, and onto map.

The construction of the dynamical sectors was first made in [5], but for completeness, we sketch this construction here. We assume now that $\lambda \in \mathcal{O} - \overline{\mathcal{M}}$ where \mathcal{M} is the McMullen domain. For such λ -values, all of the preimages of T_λ are open disks. If $\lambda \in \mathcal{O} - \overline{\mathcal{M}}$, then we may choose a circle in B_λ that is centered at the origin and mapped to a simple closed curve that lies well outside this circle. There is another circle in T_λ that is mapped to the same curve. Let R_0 be the closed portion of the sector I_0 that is contained between these two circles, and let $R_n = -R_0$.

Assume for the moment that $\lambda \notin \mathbb{R}^+$. Then the critical values do not lie in the regions R_0 or R_n , and so the critical value rays $\pm tv_\lambda$ for $t \geq 1$ (which are the images of the straight line boundaries of I_0 and I_n) do not meet R_0 or R_n . Therefore F_λ maps each of R_0 and R_n over the entire set $R_0 \cup R_n$. Moreover, each point in $R_0 \cup R_n$ has a unique preimage in R_0 as well as a similar unique preimage in R_n . Then standard arguments from complex dynamics show that the set of points whose orbits remain for all iterations in $R_0 \cup R_n$ is an invariant Cantor set on which F_λ is conjugate to the one-sided shift map on two symbols. Call this invariant set Λ_λ . By the $z \mapsto -z$ symmetry in the dynamical plane, we have that $\Lambda_\lambda = -\Lambda_\lambda$.

One checks easily that there is a fixed point p_λ in Λ_λ that lies in $R_0 \cap \partial B_\lambda$. Then $-p_\lambda$ lies in $R_n \cap \partial B_\lambda$. When n is even, $F_\lambda(-p_\lambda) = p_\lambda$ but when n is odd, $-p_\lambda$ is fixed by F_λ . These are clearly the only points in $\Lambda_\lambda \cap \partial B_\lambda$ since F_λ is conjugate to $z \mapsto z^n$ on ∂B_λ , so all other points in ∂B_λ have orbits that eventually leave $R_0 \cup R_n$. Similarly, there are a pair of preimages of $\pm p_\lambda$, one of which, q_λ , lies in $R_0 \cap \partial T_\lambda$, and the other, $-q_\lambda$, lies in $R_n \cap \partial T_\lambda$. If n is even, these points are both preimages of $-p_\lambda$, whereas, if n is odd, $-q_\lambda$ is a preimage of p_λ , and q_λ is a preimage of $-p_\lambda$. As above, these are the

only points in $\Lambda_\lambda \cap \partial T_\lambda$. Now consider the four points that are the preimages of $\pm q_\lambda$ that lie in $R_0 \cup R_n$. These four points lie on the boundaries of a pair of preimages of T_λ , one of whose centers lies in R_0 and the other in R_n . Then the eight preimages of these points lie on the boundaries of four pre-preimages of T_λ whose centers lie in R_0 or R_n . Continuing in this fashion, we find a collection of 2^j preimages of T_λ whose centers lie in $R_0 \cup R_n$ at the j^{th} stage. Here a center of a given preimage of T_λ is the unique point in this set that eventually maps onto 0. So consider the set that is the union of Λ_λ together with T_λ and all of these special preimages of T_λ . Call this set \mathcal{N} . Then \mathcal{N} is a set that is a continuous, one-to-one, onto image of the middle-thirds Cantor necklace and so \mathcal{N} is a Cantor necklace. Note that F_λ maps \mathcal{N} two-to-one over itself together with B_λ .

Let \mathcal{N}_0 be the portion of \mathcal{N} that connects the fixed point p_λ to q_λ in R_0 . \mathcal{N}_0 is also a Cantor necklace and F_λ maps \mathcal{N}_0 one-to-one over all of \mathcal{N} . Let \mathcal{N}_j be the image of \mathcal{N}_0 under the rotation $z \mapsto \omega^j z$ where $\omega = \exp(\pi i/n)$. Then F_λ also maps each \mathcal{N}_j one-to-one over \mathcal{N} .

We now define the dynamical sectors \mathcal{I}_j . The sector \mathcal{I}_j will be the region contained between the Cantor necklaces \mathcal{N}_j and \mathcal{N}_{j+1} and the portions of ∂B_λ and ∂T_λ connecting these two bounding necklaces. Thus we have that $\mathcal{I}_j = \omega^j \mathcal{I}_0$. Also, $c_0(\lambda)$ lies between \mathcal{N}_0 and \mathcal{N}_1 , so it follows that each critical point $c_j(\lambda)$ lies in the dynamical sector \mathcal{I}_j . As above, ∂B_λ and ∂T_λ meet each boundary point of the two Cantor necklaces in \mathcal{I}_j in a unique point, so the portion of the boundary of each \mathcal{I}_j in ∂B_λ and ∂T_λ is an arc.

We can easily extend the construction of the Cantor necklaces to the case where $\lambda \in \mathbb{R}^+$. In this case F_λ maps one of the boundaries of the sectors I_0 and I_n into itself, but the above construction of the Cantor set still works. The only difference is that \mathcal{N}_0 (resp., \mathcal{N}_n) now meets the real axis at the point $p_\lambda \in \mathbb{R}^+$ (resp., $-p_\lambda \in \mathbb{R}^-$), but this is the only point in $\mathcal{N}_0 \cap \mathbb{R}$ (resp.,

$\mathcal{N}_n \cap \mathbb{R}$). This defines the dynamical sectors for $\lambda \in \mathcal{O} - \overline{\mathcal{M}}$.

5 Sierpiński Curve Julia Sets

Recall that we are primarily concerned with parameters that are drawn from the main cardioids of Mandelbrot sets whose centers lie along the ring \mathcal{S}_k . All of the parameters in each of these regions correspond to maps that have an attracting cycle of some given period. So the Fatou set for these maps consists of the union of the full basins of attraction of this cycle as well as the full basin of ∞ . Our goal in this section is to prove the following result:

Theorem. *Suppose λ lies in the main cardioid of a Mandelbrot set whose center lies in the ring \mathcal{S}_k with $k \geq 2$, i.e., a Sierpiński cardioid. Then the Julia set of F_λ is a Sierpiński curve.*

Proof: By a theorem of Whyburn [18], it is known that any planar set that is compact, connected, nowhere dense, locally connected, and has the property that any two complementary domains are bounded by simple closed curves that are pairwise disjoint is homeomorphic to the Sierpiński carpet. In our case, proving four of these properties is straightforward as they follow from well known basic properties of the Julia set [13]. To be specific, since we have the Fatou domain B_λ , $J(F_\lambda)$ is not the entire Riemann sphere and therefore is compact and nowhere dense. Since the free critical orbits all tend to the attracting cycle, F_λ is hyperbolic on $J(F_\lambda)$ and hence the Julia set is locally connected. All of the components of the basins of the attracting cycles and ∞ are all open disks and so the complement of these disks, namely $J(F_\lambda)$, is a connected set.

Thus we have only to show that the boundaries of the Fatou components are simple closed curves that are pairwise disjoint. As shown in [17], ∂B_λ is a simple closed curve and so all of the boundaries of the preimages of B_λ are

also simple closed curves. The polynomial-like mapping argument in [3] that proves the existence of these Mandelbrot sets then shows that the boundaries of all the basins of the attracting cycles (as well as all of their preimages) are also simple closed curves. Hence we need only show that all of these different boundaries are pairwise disjoint.

First, since F_λ maps the critical circle strictly inside itself, we have that ∂B_λ lies outside this circle. By the H_λ symmetry in the dynamical plane, ∂T_λ then lies strictly inside this circle. So ∂B_λ and ∂T_λ are disjoint. It then follows that all of the preimages of ∂B_λ must be disjoint from one another.

Second, consider the boundaries of the preimages of the basin of the attracting cycle. Suppose that the boundaries of two of these preimages meet. Then, iterating forward, the boundaries of each of the basins of the attracting cycle must meet the boundary of at least one other such basin of the attracting cycle. In particular, the boundary of the basin that contains the critical value must meet the boundary of some other attracting basin. However, since the critical values both lie inside the curve C_{-1} , it is known [6] that there is an invariant simple closed curve ξ_0 that winds around the origin in the annulus bounded by C_0 and C_{-1} . Moreover, this curve lies in the Julia set and F_λ is conjugate to $z \mapsto z^{-n}$ on this curve. Then there is a preimage of this invariant curve ξ_{-1} that also lies in $J(F_\lambda)$ and winds around the origin in the annulus between C_{-1} and C_{-2} .

Since we are assuming that the cycle has period greater than two, the periodic critical value for the map at the center of the main cardioid of this Mandelbrot set lies on C_{-k} for some $k \geq 2$. Hence this point lies inside the curve ξ_{-1} that is contained in the annular region between C_{-2} and C_{-1} . Now points on this curve map to the invariant curve ξ_0 in the Julia set, so it follows that this scenario must hold for all parameters in the given main cardioid. But then the other attracting basin whose boundary meets that of

the basin containing the critical value must lie outside the invariant curve ξ_0 between C_0 and C_{-1} , since all of the other basins of the attracting cycle lie outside this curve. Therefore, one of the above attracting basins must pass through either ξ_0 or ξ_{-1} , which cannot happen since these curves lie in the Julia set.

Finally, the boundaries of the preimages of B_λ and the attracting basins are also disjoint. This follows since, if any two were to meet, then taking forward images of these boundaries would imply that all of the boundaries of the attracting basins would meet ∂B_λ . In particular, the attracting basin that contains the critical point would stretch all the way from ∂B_λ to ∂T_λ because of the H_λ symmetry in the dynamical plane that interchanges ∂B_λ and ∂T_λ and fixes the critical point. But then this basin would meet the invariant curve that lies in the Julia set as described above. This completes the proof.

□

In the case where the base period is two, then the two attracting basins are only separated by the invariant curve between C_0 and C_{-1} and so it is then possible for the two boundaries of the attracting basins to meet at a point in the Julia set on this curve. This does happen when the parameter lies in a period 2 bulb of a principal Mandelbrot set.

6 Precritical and Superattracting Itineraries

In this section we define itineraries of the attracting periodic orbits that are associated with parameters in the Sierpiński cardioids along each of the rings around the McMullen domain. Since the itineraries will be the same for all parameters lying in this cardioid, it will suffice to produce the itinerary for the map at the center of these cardioids, i.e., the parameters λ_ℓ^k defined in

Section 3 for which the periodic orbit is superattracting.

Recall that the dynamical sector \mathcal{I}_j contains the critical point $c_j = c_j(\lambda)$. Then we have that each of these sectors is mapped two-to-one over n adjoining sectors (plus the $n - 1$ intermediate Cantor necklaces). Specifically, the sectors $\mathcal{I}_0, \mathcal{I}_2, \dots, \mathcal{I}_{2n-2}$, are each mapped over $\cup_{j=0}^{n-1} \mathcal{I}_j$ while the other n sectors $\mathcal{I}_1, \mathcal{I}_3, \dots, \mathcal{I}_{2n-1}$ are mapped over the complementary set, $\cup_{j=n}^{2n-1} \mathcal{I}_j$.

Next recall that the curves $\gamma_k(\theta)$ are the portions of C_k defined for $0 \leq \theta \leq (n - 2)n^k\pi + \pi/n$ when $k \geq 0$. As described earlier, there is a unique point z_k in the necklace \mathcal{N}_0 for which $F_\lambda^j(z_k) \in \mathcal{N}_0$ for $j = 0, \dots, k$ and $F_\lambda^{k+1}(z_k) = 0$, i.e., the orbit of z_k lies at the centers of certain preimages of T_λ in \mathcal{N}_0 that lie outside of the first preimage of T_λ in \mathcal{N}_0 and then map closer and closer along the necklace to this preimage as j increases. As discussed in Section 3, we have that the point z_k is given by $\gamma_k(\pi/2n)$. By the $z \mapsto -z$ symmetry, the point $\gamma_k(n^k\pi + \pi/2n)$ then lies in the necklace \mathcal{N}_n for each k .

By our construction of γ_k , it follows that, for each j , there are n preimages of critical points in each of $\gamma_1 \cap \mathcal{I}_j$; n^2 second preimages of critical points in each of $\gamma_2 \cap \mathcal{I}_j$; and, in general, n^k k^{th} preimages of the critical points in $\gamma_k \cap \mathcal{I}_j$. Then, for each $k > 0$, there are exactly n^k points on the portion of γ_{-k} lying in \mathcal{I}_j that are mapped by F_λ^k to critical points. Now consider only the $n - 2$ dynamical sectors $\mathcal{I}_1, \dots, \mathcal{I}_{n-2}$ that, by construction, lie in the upper half plane. We call the $(n - 2)n^k$ preimages of the critical points under F_λ^k that lie on γ_{-k} in the sectors $\mathcal{I}_1, \dots, \mathcal{I}_{n-2}$ the *k-precritical points*.

We now assign an itinerary to each of the $(n - 2)n^k$ k -precritical points in these $n - 2$ dynamical sectors. This itinerary is a sequence of $k + 1$ digits that indicates which sector \mathcal{I}_j the successive iterates of these points lie in. So the itinerary of a k -precritical point is a sequence of the form $(s_{-k}s_{k-1}s_{k-2} \dots s_0)$ where the digit s_j implies that the corresponding point on γ_j lies in sector \mathcal{I}_{s_j} . So the given precritical point with this itinerary lies in the sector $\mathcal{I}_{s_{-k}}$;

its image lies in the sector $\mathcal{I}_{s_{k-1}}$; its second image in $\mathcal{I}_{s_{k-2}}$; and so forth until its k^{th} image is the critical point in \mathcal{I}_{s_0} .

There is one additional k -precritical point that we need to consider. This is the precritical point that lies on the real axis when $\lambda \in \mathbb{R}^+$. This orbit remains for all iterations in \mathcal{I}_0 , so its itinerary is just $(00 \dots 0)$. For all of the other itineraries, by construction, the first digit s_{-k} satisfies $1 \leq s_{-k} \leq n-2$, whereas for all subsequent digits s_j , we have $0 \leq s_j \leq 2n-1$. For example, when $n = 3$, the k -precritical points (that are not of the form $(00 \dots 0)$) all lie in \mathcal{I}_1 and the three itineraries of the 1-precritical points in γ_{-1} are 15, 14, and 13 since $F_\lambda|_{\mathcal{I}_1}$ covers $\mathcal{I}_5, \mathcal{I}_4$, and \mathcal{I}_3 . Then the nine itineraries of the 2-precritical points in γ_{-2} are

$$\begin{array}{ccc} 155 & 154 & 153 \\ 142 & 141 & 140 \\ 135 & 134 & 133. \end{array}$$

When $n = 4$, the k -precritical points now lie in $\mathcal{I}_1 \cup \mathcal{I}_2$ (excluding again $(00 \dots 0)$). The itineraries of the 1-precritical points are then 17, 16, 15, 14, 23, 22, 21, and 20. The itineraries of the 2-precritical points are then

$$\begin{array}{cccccccc} 177 & 176 & 175 & 174 & 163 & 162 & 161 & 160 \\ 157 & 156 & 155 & 154 & 143 & 142 & 141 & 140 \\ 237 & 236 & 235 & 234 & 223 & 222 & 221 & 220 \\ 217 & 216 & 215 & 214 & 203 & 202 & 201 & 200. \end{array}$$

We can obtain a list of the allowable itineraries of the k -precritical points inductively as follows. Consider the case $n = 3$. The allowable itineraries for the precritical points on γ_{-1} are, as above, 15, 14, and 13. We obtain the allowable itineraries for the precritical points on γ_{-2} by taking each allowable itinerary on γ_{-1} and adding a new final digit that corresponds to the sectors that the sector corresponding to the original final digit is mapped over. For example, \mathcal{I}_5 is mapped over $\mathcal{I}_5, \mathcal{I}_4$, and \mathcal{I}_3 , so 5 can only be followed by 5, 4, or 3. Thus we can expand 15 to 155, 154, and 153. Similarly, 4 can

only be followed by 2, 1, or 0, so 14 can be expanded to 142, 141, and 140. This produces the list of allowable itineraries above. Continuing inductively produces the list of allowable itineraries of the j -precritical points in γ_{-j} given the list in γ_{-j+1} .

Recall that, in Section 3, we showed that there was a unique parameter λ_ℓ^k for which the critical value in the upper half plane landed on the point $\gamma_{-k}(\theta)$ where $\theta = \ell\pi/3$ and $0 \leq \ell \leq 3^k$. Let us not consider the case where $\ell = 0$ since we know that this parameter lies on the real axis and the corresponding map has a superattracting periodic orbit on the positive real axis with itinerary $(0 \dots 0)$.

Proposition. *Given an allowable itinerary $s = (s_{-k}s_{k-1} \dots s_0)$ for a k -precritical point, there exists a unique parameter λ_s in $\mathcal{O} - \mathbb{R}^+$ such that the critical value in the upper half plane for the map F_{λ_s} is the k -precritical point with itinerary s .*

Proof: Since $\lambda \notin \mathbb{R}^+$, it follows that the necklaces \mathcal{N}_j for $j = 1, \dots, n-1$ always lie in the upper half plane since the sectors I_1 through I_{n-1} have this property. Thus the dynamical sectors \mathcal{I}_j for $j = 1, \dots, n-2$ always lie in the upper half plane. Let $z_s(\lambda)$ be a k -precritical point for F_λ . Then $z_s(\lambda)$ always lies in the upper half plane and varies analytically with λ . So the Proposition in Section 3 guarantees that there is a unique λ for which $v_\lambda = z_s(\lambda)$. This is the parameter λ_s . □

We now define the itineraries of the superattracting cycles for the parameters λ_s . Let $s = (s_{-k}s_{k-1} \dots s_0)$ be an allowable itinerary of a k -precritical point. Let λ_s be the parameter given in the previous Proposition and let z_s be the point with itinerary s on which the critical value in the upper half plane lands. It need not be the case that z_s lies on a superattracting periodic orbit of period $k+1$. There are two different reasons for this. We do have

that $F_{\lambda_s}^k(z_s(\lambda_s))$ is the critical point that lies in the sector \mathcal{I}_{s_0} . If s_0 is even, then F_{λ_s} maps this critical point to the critical value in the upper half plane, i.e., to the point $z_s(\lambda_s)$. Hence, in this case, we have that $z_s(\lambda_s)$ does indeed lie on a superattracting periodic orbit of period $k+1$ and the full itinerary of this orbit is $\overline{(s_{-k}s_{k-1}\dots s_0)}$. But if s_0 is odd, then the image of this critical point is the critical value in the lower half plane, namely $-z_s$, and thus z_s is not periodic with period $k+1$.

What happens in this case depends upon whether n is even or odd. If n is even, then we have that $F_{\lambda}(-z_s) = F_{\lambda}(z_s)$. So the point $-z_s$ lies on a superattracting cycle of period $k+1$. Therefore the itinerary of this orbit is $\overline{(s_{-k}^*s_{k-1}\dots s_0)}$ where $s_{-k}^* = n + s_{-k}$. For example, in the case $n = 4$, we have the 1-precritical itinerary (17). But 1 cannot follow 7 since \mathcal{I}_7 is mapped over \mathcal{I}_j where $j = 4, 5, 6$, or 7. Therefore, this precritical itinerary can be replaced with (57) which does correspond to a superattracting cycle of period 2. Similarly, the 2-precritical itinerary (177) can be replaced with (577) to get an itinerary of a superattracting cycle. In general, for any k -precritical itinerary that ends in an odd number, the first digit s_{-k} should be replaced by $n + s_{-k}$ to get the itinerary of the superattracting cycle.

If n is odd, then, by the $z \mapsto -z$ symmetry, the orbit of $-z_s$ is symmetric with the orbit of z_s . That is, $F_{\lambda_s}^{k+1}(-z_s) = z_s$. Hence z_s lies on a superattracting cycle of period $2(k+1)$ and its itinerary is $\overline{(s_{-k}s_{k-1}\dots s_0s_{-k}^*s_{k-1}^*\dots s_0^*)}$ where now $s_j^* = s_j + n \bmod 2n$. For example, in the case $n = 3$, we have the 1-precritical itinerary (15). Again, 1 cannot follow 5, but 4 can. The precritical itinerary corresponding to the negative of this point is then (42). So we can replace the precritical itinerary (15) with (1542) which corresponds to a superattracting cycle of period 4. Similarly, the 2-precritical itinerary (155) can be replaced by (155422) which now corresponds to a superattracting cycle of period 6.

7 The Dynamical Invariant

In the previous section, we assigned an itinerary to the superattracting cycle associated to a parameter that lies at the center of each Sierpiński cardioid attached to the rings \mathcal{S}_k surrounding the McMullen domain. As we showed, each of these itineraries was a different sequence. Now we know that certain of these superattracting parameters have conjugate dynamics. Since the superattracting cycles for two such conjugate maps F_λ and F_μ are preserved by the conjugacy, it would be nice if the corresponding superattracting itineraries were the same. However this is not true in general. To remedy this, we will use the techniques introduced in Section 4 to construct additional invariant Cantor necklaces \mathcal{N}^j where \mathcal{N}^0 is the original Cantor necklace \mathcal{N} .

Recall that if $\lambda \notin \mathbb{R}^+$, then the fact that the critical values do not lie in R_0 or R_n , combined with the existence of a fixed point $p_\lambda^0 = p_\lambda$ in $R_0 \cap \partial B_\lambda$, yielded the invariant Cantor necklace $\mathcal{N} = \mathcal{N}^0$ in $R_0 \cup R_n \cup T_\lambda$. Now, since F_λ is conjugate to $z \mapsto z^n$ on ∂B_λ , ∂B_λ contains exactly $n - 1$ fixed points. In [14], Moreno Rocha gives a formula for the locations of these fixed points in terms of the symmetry sector in parameter space in which λ lies. Recall that these $n - 1$ symmetry sectors are given by \mathcal{P}_j for $j = 0, \dots, n - 2$ where $\lambda \in \mathcal{P}_j$ if

$$\frac{2j\pi}{n-1} \leq \text{Arg } \lambda < \frac{2(j+1)\pi}{n-1}.$$

Then, if $\lambda \in \mathcal{P}_k$, the results in [14] show that $R_j \cap \partial B_\lambda$ contains exactly one fixed point if:

- $j=0$, or
- j is even with $0 < j < k + 1$ or $k + 1 + n < j < 2n - 1$, or
- j is odd with $k + 1 < j < k + 1 + n$.

We call R_j with j as above a *fixed point sector*. Moreover, the critical values $\pm v_\lambda$ lie in the *critical value sectors* R_{k+1} and R_{k+1+n} , so no critical value sector is a fixed point sector.

It is clear then that, for $\lambda \in \mathcal{P}_k$, all $n - 1$ fixed points in ∂B_λ yield invariant Cantor necklaces contained within the union of its corresponding fixed point sector R_j and the antipodal sector R_{j+n} . When n is odd, opposite fixed points on ∂B_λ will correspond to the same necklace, so that we have $n - 1$ invariant Cantor necklaces when n is even and $(n - 1)/2$ when n is odd. We denote these necklaces by \mathcal{N}^l , where $l \in \{1, \dots, n - 1\}$ (where \mathcal{N}^l coincides with $\mathcal{N}^{-l \bmod (n-1)}$ if n is odd), and $p_\lambda^l \in \mathcal{N}^l$ is the l^{th} fixed point in B_λ counting counter-clockwise from p_λ^0 .

Following the construction in Section 4, let \mathcal{N}_0^l be the portion of \mathcal{N}^l extending from p_λ^l to the fixed point preimage on ∂T_λ lying in the same fixed point sector as p_λ^l . Then let \mathcal{N}_j^l for $j \in \{1, \dots, 2n - 1\}$ be the image of \mathcal{N}_0^l under the rotation $z \mapsto \omega^j z$, where $\omega = \exp(\pi i/n)$. This then gives an alternate partition into dynamical sectors \mathcal{I}_j^l , where \mathcal{I}_j^l is the region between \mathcal{N}_j^l and \mathcal{N}_{j+1}^l , and the portions of ∂B_λ and ∂T_λ connecting these bounding necklaces.

We can then define an itinerary for the k -precritical points with respect to any one of these new partitions. For a given k -precritical point, the $n - 1$ or $(n - 1)/2$ (depending on the parity of n) itineraries produced usually bear no relation to one another. Moreover, if F_λ and F_μ are critically finite and conjugate, as described in the Introduction and proved in [11], we know that the conjugacy is given by a rotation, or a rotation composed with complex conjugation. If the conjugacy is given by a rotation, the itinerary for F_λ will not be the same as the itinerary for F_μ as defined in Section 6, but will coincide with the itinerary for F_μ *with respect to a different partition* (suitably relabeled). If the conjugacy is given by a rotation and complex

conjugation, then the itinerary for F_λ will be related in a nice way to the itinerary for F_μ with respect to a relabeling of a new partition. Thus to construct an actual conjugacy invariant, we must canonically choose one of the invariant Cantor necklaces for each parameter, and use its corresponding partition to define the itinerary. We make this precise below.

If $\lambda \in \mathcal{P}_0$ is a superattracting parameter on \mathcal{S}_i , then we associate the same itinerary to λ as in the previous section, using the partition associated to \mathcal{N}^0 . Now, as shown in [11], two critically finite parameters μ and λ are known to have conjugate dynamics if and only if $\mu = \nu^{2j}\lambda$ or $\mu = \nu^{2j}\bar{\lambda}$ for some $j \in \mathbb{Z}$, where ν is a primitive $n - 1^{\text{st}}$ root of unity. Thus, if $\mu \in \mathcal{P}_k$ is a superattracting parameter on \mathcal{S}_i , there exist either one (if n is odd) or two (if n is even) parameters $\lambda \in \mathcal{P}_0 \cap \mathcal{S}_i$ with F_λ conjugate to F_μ . This is because both $\lambda_1 = \nu^{-k}\mu$ and $\lambda_2 = \nu^{k+1}\bar{\mu}$ lie in \mathcal{P}_0 . When n is odd, only F_{λ_1} is conjugate to F_μ if k is even, and only F_{λ_2} is conjugate to F_μ if k is odd. But when n is even, both F_{λ_1} and F_{λ_2} are conjugate to F_μ regardless of the parity of k , since $\nu^{-k} = \nu^{n-k-1}$, and $\nu^{k+1} = \nu^{k+n}$, and one of each pair $(-k, n - k - 1)$ and $(k + 1, k + n)$ will always be an even power of ν .

Now suppose $\mu \in \mathcal{P}_k$. Let λ be the parameter in \mathcal{P}_0 with F_μ conjugate to F_λ , choosing the one of smaller argument if n is even. Let p_μ^m be the fixed point in ∂B_μ sent to p_λ^0 under the conjugacy. Assign to μ the itinerary for F_μ obtained via the necklace \mathcal{N}^m , relabeled so that the sector adjacent to p_μ^m in the counter-clockwise direction is \mathcal{I}_0^m . Call two itineraries $(a_1 a_2 a_3 \dots)$ and $(b_1 b_2 b_3 \dots)$ “*complex conjugate*” if the corresponding symbols are related by $a_j + b_j = 2n - 1 \pmod{2n}$. Note an itinerary is transformed into its conjugate by relabeling the partition in the opposite (clockwise) direction. Thus any two superattracting parameters with conjugate maps will have either the same itinerary, or conjugate itineraries if the conjugacy is given by a composition of rotation and complex conjugation.

The one exception to this occurs again when $\lambda_0 \in \mathbb{R}^+$, since the parameter $\nu\bar{\lambda}_0 = \nu\lambda_0$ now lies in the symmetry sector \mathcal{P}_1 . Hence the itinerary $\overline{(00\dots 00)}$ is unique in this respect.

This enables us to produce a list of all the superattracting itineraries corresponding to parameters lying in the main cardioids of Mandelbrot sets attached to the ring \mathcal{S}_k by simply listing the itineraries corresponding to parameters in \mathcal{P}_0 modulo the above constraints. For example, the superattracting itineraries with base period 3 when $n = 3$ are given by

$$\overline{(000)}, \overline{(155422)}, \overline{(154)}, \overline{(153420)}, \overline{(142)}, \overline{(141414)}.$$

while the corresponding itineraries for the case $n = 4$ are

$$\overline{(000)}, \overline{(577)}, \overline{(176)}, \overline{(575)}, \overline{(174)}, \overline{(563)}.$$

The complex conjugate itineraries when $n = 4$ are then given by

$$\overline{(200)}, \overline{(601)}, \overline{(202)}, \overline{(603)}, \overline{(214)}.$$

This produces a dynamical invariant that differentiates the non-conjugate parameters in the cardioids along the rings \mathcal{S}_k .

Finally, this gives a count of the number of conjugacy classes of maps in the Sierpiński cardioids attached to \mathcal{S}_k .

Proposition. *The number of conjugacy classes of maps drawn from the Sierpiński cardioids along \mathcal{S}_k is*

$$\frac{(n-2)n^k + 1}{n-1} + 1$$

if n is odd and

$$\frac{(n-2)n^k + n}{2(n-1)}$$

if n is even.

Proof: When n is odd, the number of parameters in the symmetry sector \mathcal{P}_0 is $((n-2)n^k+1)/(n-1)$. But this does not count the parameter $\nu\lambda$ where $\lambda \in \mathbb{R}^+$, which is then the only other conjugacy class. So we add 1 to the above count to get the number of conjugacy classes when n is odd.

When n is even, the number of parameters in the symmetry sector \mathcal{P}_0 is again $((n-2)n^k+1)/(n-1)$. The map corresponding to a parameter along \mathbb{R}^+ is not conjugate to any other map in this symmetry sector. However, any other parameter λ in this sector is conjugate to $\nu\bar{\lambda}$, which also lies in \mathcal{P}_0 . Therefore the count of the number of conjugacy classes in this case is

$$\frac{\frac{(n-2)n^k+1}{n-1}+1}{2} = \frac{(n-2)n^k+n}{2(n-1)}.$$

□

8 Final Comments

In this paper we have proved that the Julia sets arising from Sierpiński cardioids attached to the rings \mathcal{S}_k for $k \geq 2$ are all Sierpiński curves. This is not necessarily the case when $k < 2$. For example, when $k = 0$, there are $n-1$ cardioids of the principal Mandelbrot sets that the ring \mathcal{S}_0 passes through. However, it is known that the Julia sets arising from parameters in these regions are very different: they are so-called checkerboard Julia sets [1]. In this case, the boundaries of the basins of attraction of the attracting cycles now meet the boundaries of the preimages of B_λ at infinitely many points, although these boundaries of the basins of attraction never touch each other. Thus these sets are not Sierpiński curves.

When $k = 1$, as mentioned earlier, the ring \mathcal{S}_1 now passes through $n-1$ period 2 bulbs of the principal Mandelbrot sets. In these cases, the corresponding Julia sets now contain Fatou domains that are homeomorphic to

the “basilica,” i.e., the filled Julia set for $z^2 - 1$. As a consequence, infinitely many of the boundaries of the basins of the attracting cycle now touch each other, so again the Julia set is not a Sierpiński curve.

References

- [1] Blanchard, P., Cilingir, F., Cuzzocreo, D., Devaney, R. L., Look, D. M., and Russell, E. D. Checkerboard Julia Sets for Rational Maps. *International Journal of Bifurcation and Chaos* **23** (2013).
- [2] Devaney, R. L. Structure of the McMullen Domain in the Parameter Space of Rational Maps. *Fundamenta Mathematicae* **185** (2005), 267-285.
- [3] Devaney, R. L. The McMullen Domain: Satellite Mandelbrot Sets and Sierpiński Holes. *Conformal Geometry and Dynamics* **11** (2007), 164-190.
- [4] Devaney, R. L. Mandelbrot Sets Adorned with Halos in Families of Rational Maps. In *Complex Dynamics: Twenty-Five Years after the Appearance of the Mandelbrot Set*. American Math Society, Contemporary Math **396** (2006), 37-50.
- [5] Devaney, R. L. Cantor Necklaces and Structurally Unstable Sierpiński Curve Julia Sets for Rational Maps. *Qualitative Theory of Dynamical Systems* **5** (2006), 337-359.
- [6] Devaney, R. L. Cantor Sets of Circles of Sierpiński Curve Julia Sets. *Ergodic Theory and Dynamical Systems* **27** (2007), 1525-1539.
- [7] Devaney, R. L. Singular Perturbations of Complex Polynomials. *Bulletin of the AMS* **50** (2013), 391-429.

- [8] Devaney, R. L. and Look, D. M. Buried Sierpiński Curve Julia Sets. *Discrete and Continuous Dynamical Systems* **13** (2005), 1035-1046.
- [9] Devaney, R. L., Look, D. M., and Uminsky, D. The Escape Trichotomy for Singularly Perturbed Rational Maps. *Indiana University Mathematics Journal* **54** (2005), 1621-1634.
- [10] Devaney, R. L. and Marotta, S. The McMullen Domain: Rings Around the Boundary. *Transactions of the AMS* **359** (2007), 3251-3273.
- [11] Devaney, R. L. and Pilgrim, K. Dynamic Classification of Escape Time Sierpiński Curve Julia Sets. *Fundamenta Mathematicae* **202** (2009), 181-198.
- [12] McMullen, C. The Classification of Conformal Dynamical Systems. *Current Developments in Mathematics*. International Press, Cambridge, MA, (1995), 323-360.
- [13] Milnor, J. *Dynamics in One Complex Variable*. Third Edition. Annals of Mathematics Studies. Princeton University Press, (2006).
- [14] Moreno Rocha, M. A Combinatorial Invariant for Escape Time Sierpiński Rational Maps. *Fundamenta Mathematicae* **222** (2013), 99-130.
- [15] Roesch, P. On Capture Zones for the Family $f_\lambda(z) = z^2 + \lambda/z^2$. In *Dynamics on the Riemann Sphere*. European Mathematical Society, (2006), 121-130.
- [16] Qiu, W., Roesch, P., Wang, Z., and Yin, Y. Hyperbolic Components of McMullen Maps. To appear.

- [17] Qiu, W., Wang, Z., and Yin, Y. Dynamics of McMullen Maps. *Advances in Math.* **229** (2012), 2525-2577.
- [18] Whyburn, G. T. Topological Characterization of the Sierpiński Curve. *Fundamenta Mathematicae* **45** (1958), 320-324.